JCI The Journal of Clinical Investigation

Hepatitis B virus X protein represses miRNA-148a to enhance tumorigenesis

Xiaojie Xu, … , Nan Du, Qinong Ye

J Clin Invest. 2013;123(2):630-645. https://doi.org/10.1172/JCI64265.

Research Article **Oncology**

MicroRNAs (miRNAs) have been shown to be dysregulated in virus-related cancers; however, miRNA regulation of virus-related cancer development and progression remains poorly understood. Here, we report that miR-148a is repressed by hepatitis B virus (HBV) X protein (HBx) to promote cancer growth and metastasis in a mouse model of hepatocellular carcinoma (HCC). Hematopoietic pre–B cell leukemia transcription factor–interacting protein (HPIP) is an important regulator of cancer cell growth. We used miRNA target prediction programs to identify miR-148a as a regulator of HPIP. Expression of miR-148a in hepatoma cells reduced HPIP expression, leading to repression of AKT and ERK and subsequent inhibition of mTOR through the AKT/ERK/FOXO4/ATF5 pathway. HBx has been shown to play a critical role in the molecular pathogenesis of HBV-related HCC. We found that HBx suppressed p53-mediated activation of miR-148a. Moreover, expression of miR-148a was downregulated in patients with HBV-related liver cancer and negatively correlated with HPIP, which was upregulated in patients with liver cancer. In cultured cells and a mouse xenograft model, miR-148a reduced the growth, epithelial-to-mesenchymal transition, invasion, and metastasis of HBx-expressing hepatocarcinoma cells through inhibition of HPIP-mediated mTOR signaling. Thus, miR-148a activation or HPIP inhibition may be a useful strategy for cancer treatment.

Hepatitis B virus X protein represses miRNA-148a to enhance tumorigenesis

Xiaojie Xu,[1,2] Zhongyi Fan,[1,3] Lei Kang,[1,4] Juqiang Han,[1,5] Chengying Jiang,[1,6] Xiaofei Zheng,[7] Ziman Zhu,[3] Huabo Jiao,[3] Jing Lin,[3] Kai Jiang,[1] Lihua Ding,[1] Hao Zhang,[1] Long Cheng,[1] Hanjiang Fu,[7] Yi Song,[7] Ying Jiang,[7] Jiahong Liu,[1,3] Rongfu Wang,[4] Nan Du,[3] and Qinong Ye[1,2]

[1]Department of Medical Molecular Biology, Beijing Institute of Biotechnology, Beijing, People's Republic of China. [2]Institute of Cancer Stem Cell, Cancer Center, Dalian Medical University, Liaoning, People's Republic of China. [3]First Affiliated Hospital, Chinese PLA General Hospital, Beijing, People's Republic of China. [4]Department of Nuclear Medicine, Peking University First Hospital, Beijing, People's Republic of China. [5]Institute of Hepatology, Beijing Military General Hospital, Beijing, People's Republic of China. [6]Department of Pathology, Chinese PLA General Hospital, Beijing, People's Republic of China. [7]Beijing Institute of Radiation Medicine, Beijing, People's Republic of China.

MicroRNAs (miRNAs) have been shown to be dysregulated in virus-related cancers; however, miRNA regulation of virus-related cancer development and progression remains poorly understood. Here, we report that miR-148a is repressed by hepatitis B virus (HBV) X protein (HBx) to promote cancer growth and metastasis in a mouse model of hepatocellular carcinoma (HCC). Hematopoietic pre–B cell leukemia transcription factor–interacting protein (HPIP) is an important regulator of cancer cell growth. We used miRNA target prediction programs to identify miR-148a as a regulator of HPIP. Expression of miR-148a in hepatoma cells reduced HPIP expression, leading to repression of AKT and ERK and subsequent inhibition of mTOR through the AKT/ERK/FOXO4/ATF5 pathway. HBx has been shown to play a critical role in the molecular pathogenesis of HBV-related HCC. We found that HBx suppressed p53-mediated activation of miR-148a. Moreover, expression of miR-148a was downregulated in patients with HBV-related liver cancer and negatively correlated with HPIP, which was upregulated in patients with liver cancer. In cultured cells and a mouse xenograft model, miR-148a reduced the growth, epithelial-to-mesenchymal transition, invasion, and metastasis of HBx-expressing hepatocarcinoma cells through inhibition of HPIP-mediated mTOR signaling. Thus, miR-148a activation or HPIP inhibition may be a useful strategy for cancer treatment.

Introduction

MicroRNAs (miRNAs) are small noncoding RNA molecules that inhibit gene expression by interacting preferentially with the 3′-untranslated regions (3′-UTRs) of target mRNAs (1, 2). These interactions may cause either inhibition of translation of the targeted mRNAs or their degradation. miRNAs have been shown to exhibit regulatory functions in numerous cellular processes, including proliferation, differentiation, and apoptosis. Accumulating evidence indicates that dysregulated miRNA expression is a common feature of human tumors (3). miRNAs can function as either oncogenes or tumor suppressors through the suppression of key protein-coding genes involved in cancer development and progression (4). Thus, they are involved in the regulation of many cancer-related signaling pathways, including the mTOR signaling pathway, which is commonly deregulated in human cancers (5). PKB/AKT and ERK can activate the mTOR kinase (6, 7). The activated mTOR kinase phosphorylates 2 key translational regulators, p70 ribosomal S6 kinase 1 (S6K1), which is a positive regulator of protein synthesis, and eukaryotic initiation factor 4E–binding (eIF4E-binding) protein 1 (4E-BP1), which negatively regulates eIF4E, a key rate-limiting initiation factor for cap-dependent translation. 4E-BP1 phosphorylation releases eIF4E, allowing translation initiation. Phosphorylation of S6K1 and 4E-BP1 leads to activation of their downstream effectors, including cyclin D1 and the oncoprotein c-myc.

It has been estimated that 10% to 15% of cancers are caused by viral infections (8, 9). The most common are liver cancer caused by persistent infection with hepatitis B virus (HBV) or hepatitis C virus and cervical cancer caused by human papilloma virus. Recently, cellular miRNA expression has been shown to be interfered in response to virus infection (10). For example, by analyzing miRNA expression change profiles, Zhang et al. compared the miRNA expression alterations during HBV infection with those in patients with hepatocellular carcinoma (HCC) (11). Alteration of miRNA expression during chronic HBV infection was closer to that in patients with HCC than that during acute HBV infection, suggesting the contribution of altered miRNAs to HCC genesis from chronic HBV infection. Although cellular miRNAs were shown to be regulated by viruses, how perturbation of cellular miRNAs influences cancer development and progression remains largely unknown.

We and others have previously shown that hematopoietic pre–B cell leukemia transcription factor–interacting (PBX-interacting) protein (HPIP) can regulate cancer cell growth through activation of AKT and ERK (12, 13). HPIP is a corepressor for the transcription factor PBX, which is involved in organogenesis and tumorigenesis (14). HPIP interacts with estrogen receptor (ER) and recruits Src kinase and the p85 subunit of PI3K to estrogen-ER complex, which in turn activates AKT and ERK1/2 (13, 15). Activation of AKT and ERK1/2 leads to enhanced ER phosphorylation and estrogen-responsive gene expression (12). The HPIP-ER interaction in breast cancer cells promotes proliferation, in vitro migration and in vivo tumor growth. To further study the role of HPIP in cancer, we screened a series of miRNAs and identified HPIP as the target of miR-148a, which has been reported to be downregulated

Authorship note: Xiaojie Xu, Zhongyi Fan, and Lei Kang contributed equally to this work.

Conflict of interest: The authors have declared that no conflict of interest exists.

Citation for this article: *J Clin Invest.* 2013;123(2):630–645. doi:10.1172/JCI64265.

in gastric cancer (16), colorectal cancer (16), and pancreatic ductal adenocarcinoma (17). We show that miR-148a, by targeting HPIP, reduces the growth, epithelial-to-mesenchymal transition (EMT), invasion, and metastasis of hepatocarcinoma cells through the inhibition of the AKT/mTOR or ERK/mTOR pathway. Moreover, HBV X protein (HBx), a virally encoded protein playing a key role in the molecular pathogenesis of HBV-related HCC (18, 19), suppresses cellular miR-148a expression through interaction with the tumor suppressor p53, thus linking the miR-148a/HPIP/mTOR pathway to virus-related tumor growth and metastasis.

Results

miR-148a downregulates HPIP expression by targeting its 3′-UTR. To further investigate the role of HPIP in cancer, we used 2 target prediction programs, TargetScan and miRanda, to screen for miRNAs that target HPIP. Our analysis predicted 3 potential HPIP-targeting miRNAs, miR-148a, miR-148b, and miR-152. Western blot analysis showed that only miR-148a could inhibit HPIP expression in HepG2 hepatoma cells (Figure 1A, Supplemental Figure 1, and Supplemental Figure 2A; supplemental material available online with this article; doi:10.1172/JCI64265DS1). Moreover, miR-148a overexpression also decreased HPIP expression in BEL-7402, SMMC-7721, and MHCC97-H hepatoma cells (Figure 1A). In contrast, inhibition of miR-148a increased HPIP expression in the above-mentioned cell lines (Figure 1B). miR-148a modulated only the protein level but not the mRNA level of HPIP, suggesting that this regulation is posttranscriptional (Supplemental Figure 2B).

To confirm whether HPIP is a direct and specific target of miR-148a, we transfected HepG2 cells with HPIP 3′-UTR or 3′-UTR mutated luciferase reporter and the expression plasmid for miR-148a, miR-148b, or miR-152. miR-148a, but not miR-148b and miR-152, decreased the HPIP 3′-UTR reporter activity, suggesting that miR-148a specifically targets HPIP (Figure 1C). miR-148a did not affect the luciferase activity of the mutant reporter in which the binding sites for miR-148a were mutated. Similar results were obtained in BEL-7402 and SMMC-7721 cells (Supplemental Figure 2, C and D) as well as normal human hepatocyte LO2 cells (Figure 1D). Taken together, these results suggest that miR-148a inhibits HPIP expression by directly targeting its 3′-UTR.

miR-148a represses activation of AKT and ERK through inhibition of HPIP. HPIP has been shown to activate AKT and ERK in MCF7 breast cancer cells through its interaction with Src kinase and the p85 subunit of PI3K (13). Thus, we tested whether HPIP interacts with Src and the p85 subunit of PI3K in hepatoma cells. Coimmunoprecipitation experiments showed that HPIP also associated with p85 and Src in HepG2 hepatoma cells (Supplemental Figure 3A).

Activation of PI3K has been shown to produce phosphatidylinositol-3,4-bisphosphate and phosphatidylinositol-3,4,5-triphosphate that bind to the pleckstrin homology domain of AKT and 3′-phosphoinositide-dependent kinase-1 (PDK1), leading to their translocation to the plasma membrane (20). The colocalization of activated PDK1 and AKT allows AKT to become phosphorylated by PDK1 at threonine 308 (T308). AKT can also be phosphorylated at serine 473 (S473) by the mTORC2 complex of the mTOR protein kinase. Src has been shown to activate ERK1/2 through the Ras/Raf/MEK1/2 pathway. As expected, HPIP activated AKT and ERK1/2 in HepG2 cells (Supplemental Figure 3, B and C). The role of HPIP in the regulation of AKT had phosphorylation site specificity, because HPIP increased the level of AKT phosphorylation on T308 but not on S473. Moreover, the PI3K inhibitor wortmannin inhibited the HPIP-mediated activation of AKT (Supplemental Figure 3B), and the Src kinase inhibitor PP2 repressed the HPIP-mediated activation of ERK1/2 (Supplemental Figure 3C), suggesting that HPIP activates AKT and ERK through its interaction with p85 and Src in hepatoma cells.

Since miR-148a inhibits HPIP expression, we determined whether miR-148a represses activation of AKT and ERK through inhibition of HPIP. Western blot analysis showed that miR-148a overexpression in HepG2 cells decreased the phosphorylation levels of AKT and ERK1/2, whereas knockdown of miR-148a with miR-148a inhibitor enhanced AKT and ERK1/2 phosphorylation, though their total levels remained unchanged (Figure 2A). Like HPIP, miR-148a only inhibited the level of AKT phosphorylation on T308.

Next, we examined whether miR-148a inhibition of AKT and ERK was due to the inhibition of HPIP. We transfected miR-148a–expressing HepG2 (miR-148a-HepG2) cells with HPIP or HPIP siRNA. As expected, HPIP reexpression in miR-148a-HepG2 cells reversed the inhibition of AKT and ERK mediated by miR-148a (Figure 2B), and HPIP knockdown abolished the ability of miR-148a to repress AKT and ERK (Supplemental Figure 4). The knockdown effects could be rescued by siRNA-resistant HPIP expression. In addition, HPIP knockdown had similar effects to miR-148a overexpression on regulation of AKT and ERK (Supplemental Figure 4). These data suggest that miR-148a represses AKT and ERK through the inhibition of HPIP.

miR-148a suppresses the mTOR pathway through inhibition of HPIP/AKT and HPIP/ERK pathways. Given that AKT and ERK can activate the mTOR pathway (6, 7) and miR-148a represses activation of AKT and ERK, we decided to investigate whether miR-148a represses the mTOR pathway. Western blot analysis showed that, consistent with the results of miR-148a inhibition of AKT and ERK phosphorylation, miR-148a overexpression in HepG2 cells decreased the levels of total mTOR and phosphorylation of mTOR and phosphorylation of S6K1 and 4E-BP1, 2 mTOR kinase targets, as well as the mTOR downstream effectors c-myc and cyclin D1, whereas knockdown of miR-148a with miR-148a inhibitor had opposite effects (Figure 2A).

Next, we determined whether miR-148a inhibition of the mTOR pathway was due to the inhibition of HPIP. We transfected miR-148a-HepG2 cells with HPIP or HPIP siRNA. Indeed, HPIP reexpression in miR-148a-HepG2 cells reversed the inhibition of the mTOR pathway mediated by miR-148a (Figure 2B), and HPIP knockdown abolished the ability of miR-148a to suppress the mTOR pathway (Supplemental Figure 4). The knockdown effects could be rescued by siRNA-resistant HPIP expression. Moreover, HPIP knockdown had similar effects to miR-148a overexpression on the regulation of the mTOR pathway (Supplemental Figure 4). These results indicate that miR-148a suppresses the mTOR pathway through the inhibition of HPIP.

To further determine whether miR-148a represses the mTOR pathway through inhibition of HPIP-mediated activation of ERK, AKT, and mTOR, we treated HPIP-transfected HepG2 cells with PD98059, LY294002, and rapamycin, which are MAPK/ERK1/2, PI3K/AKT, and mTOR pathway inhibitors, respectively. Intriguingly, inhibition of ERK1/2, AKT, and mTOR by PD98059, LY294002, and rapamycin, respectively, abolished the ability of HPIP to activate ERK, AKT, and mTOR as well as mTOR targets (Figure 2C). Furthermore, AKT or ERK reexpression in miR-148a-HepG2 cells reversed the inhibition of the

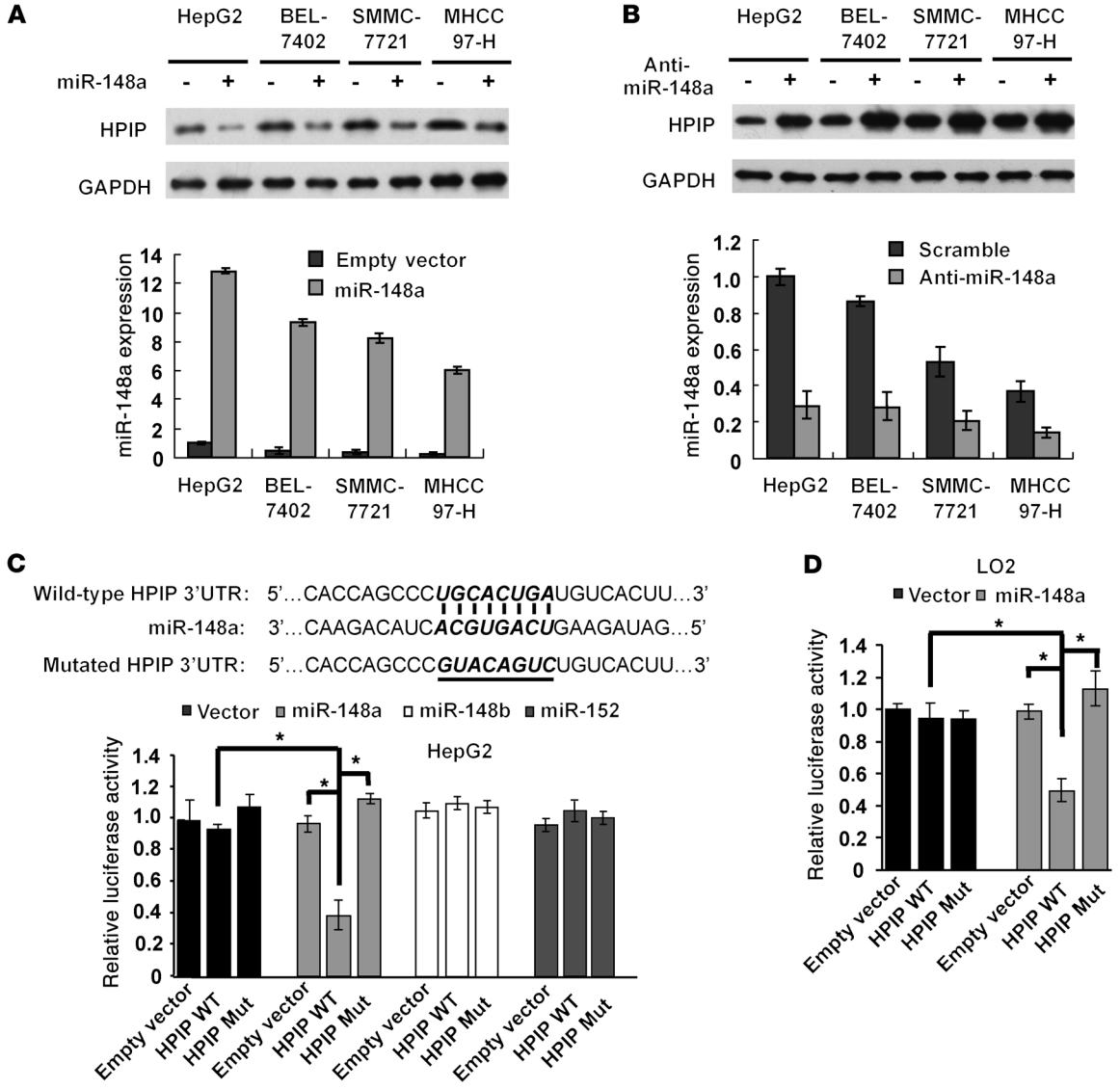

Figure 1

miR-148a inhibits HPIP expression by targeting its 3′-UTR. (**A** and **B**) Immunoblot analysis of the indicated HCC cell lines transfected with (**A**) miR-148a or (**B**) anti–miR-148a. Histograms under the immunoblot graphs show corresponding miR-148a expression levels by real-time RT-PCR. (**C**) miRNA luciferase reporter assays in HepG2 cells transfected with wild-type or mutated HPIP reporter and miR-148a, miR-148b, or miR-152. The top panel indicates wild-type and mutant forms of putative miR-148a target sequences of HPIP 3′-UTR. Bold and italicized font indicates the putative miR-148a–binding sites within human HPIP 3′-UTR. Underlining indicates the mutations introduced into the HPIP 3′-UTR. HPIP WT, wild-type HPIP 3′-UTR; HPIP Mut, mutated HPIP 3′-UTR. (**D**) miRNA luciferase reporter assays in LO2 cells transfected with miR-148a and wild-type or mutated HPIP reporter. All values shown are mean ± SD of triplicate measurements and have been repeated 3 times with similar results (*$P < 0.01$).

mTOR pathway mediated by miR-148a (Supplemental Figure 5, A–C), and the inhibition of AKT and ERK by LY294002 and PD98059 abolished the ability of miR-148a to repress mTOR signaling (Supplemental Figure 5D). It should be noted that PD98059, LY294002, and rapamycin at relatively high concentrations inhibited the expression of total mTOR, but low concentrations of PD98059, LY294002, and rapamycin did not (Figure 2, C and D). Taken together, our data suggest that miR-148a represses the mTOR pathway through inhibition of HPIP-mediated activation of ERK and AKT.

mTOR exists in 2 distinct complexes: mTORC1 and mTORC2 (21). mTORC1 is highly sensitive to rapamycin, whereas mTORC2 is relatively insensitive to rapamycin. The role of the mTORC2 complex, which is based on the interaction between mTOR and rapamycin-insensitive companion of mTOR (Rictor), has only recently emerged in cancer cell biology and is mainly related to the regulation of AKT S473 phosphorylation. The fact that miR-148a inhibits mTOR expression raises the possibility that mTOR might be a direct target of miR-148a. We used 2 target prediction programs, TargetScan and miRanda, to screen for miRNAs that target

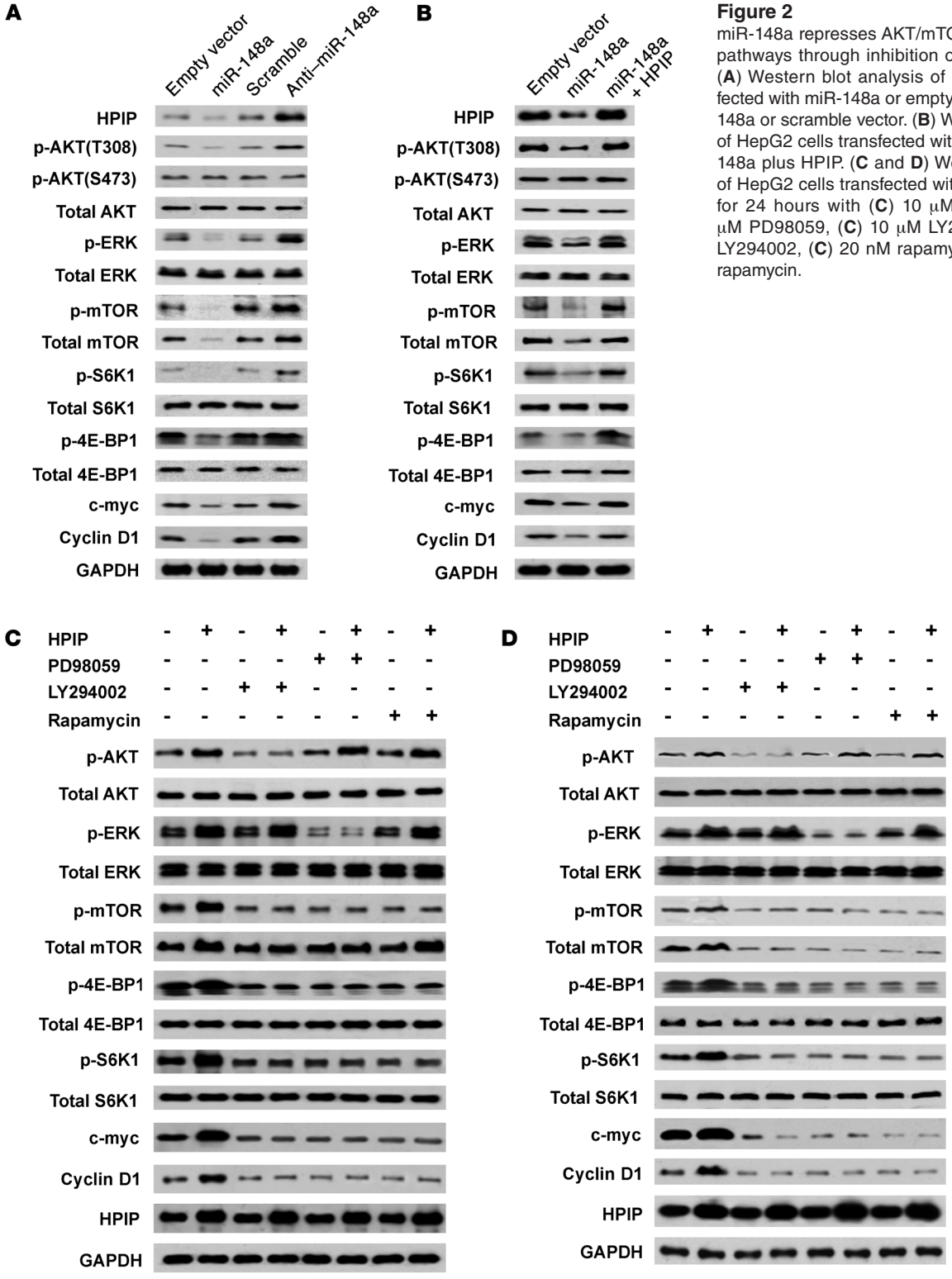

Figure 2
miR-148a represses AKT/mTOR and ERK/mTOR pathways through inhibition of HPIP expression. (**A**) Western blot analysis of HepG2 cells transfected with miR-148a or empty vector or anti–miR-148a or scramble vector. (**B**) Western blot analysis of HepG2 cells transfected with miR-148a or miR-148a plus HPIP. (**C** and **D**) Western blot analysis of HepG2 cells transfected with HPIP and treated for 24 hours with (**C**) 10 μM PD98059, (**D**) 40 μM PD98059, (**C**) 10 μM LY294002, (**D**) 50 μM LY294002, (**C**) 20 nM rapamycin, or (**D**) 200 nM rapamycin.

mTOR. However, our analysis did not predict mTOR as a direct target of miR-148a. To further test whether mTOR is as good a direct target of miR-148a as HPIP, we transfected HepG2 cells with mTOR 3′-UTR luciferase reporter and the expression plasmid for miR-148a. The results showed that miR-148a did not decrease the mTOR 3′-UTR reporter activity, suggesting that mTOR is not a direct target of miR-148a (Supplemental Figure 6A). As mentioned above, miR-148a has little effect on AKT S473 phosphorylation activated by mTORC2, although it alters the expression of mTOR. To further determine whether miR-148a/HPIP regulates mTOR

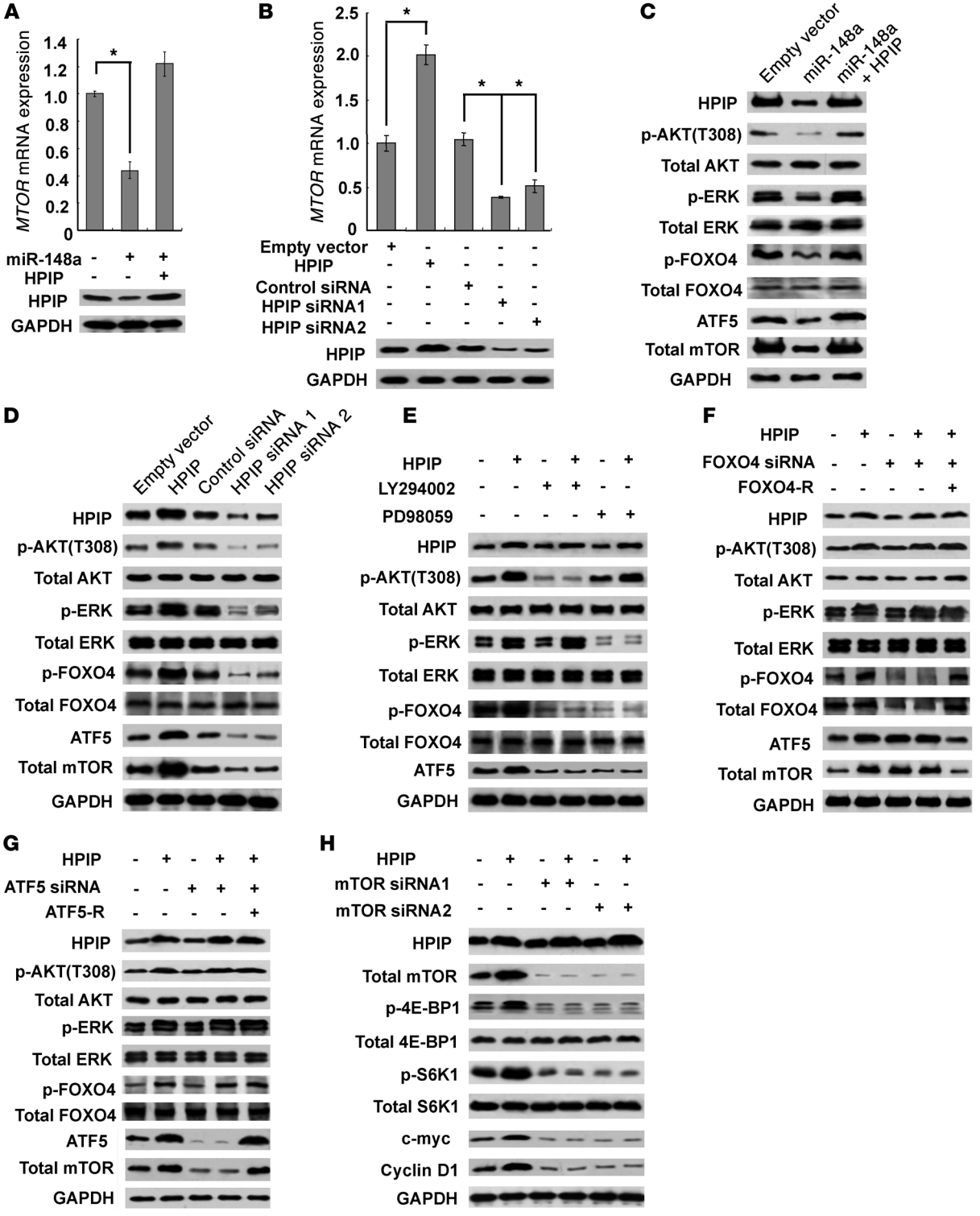

Figure 3

miR-148a/HPIP regulates mTOR expression through the AKT/ERK/FOXO4/ATF5 pathway. (**A**) HepG2 cells were transfected with miR-148a or miR-148a plus HPIP and analyzed for *MTOR* mRNA expression by real-time RT-PCR and for HPIP expression by immunoblot. All values shown are mean ± SD of triplicate measurements and have been repeated 3 times with similar results (*$P < 0.01$). (**B**) HepG2 cells were transfected with HPIP or HPIP siRNAs and analyzed as in **A**. (**C**) Western blot analysis of HepG2 cells transfected with miR-148a or miR-148a plus HPIP. (**D**) Western blot analysis of HepG2 cells transfected with HPIP or HPIP siRNAs. (**E**) Immunoblot analysis of HepG2 cells transfected with HPIP and treated for 24 hours with 10 μM PD98059 or 10 μM LY294002. (**F** and **G**) Immunoblot analysis of HepG2 cells transfected with the indicated constructs. (**F**) siRNA-resistant FOXO4 (FOXO4-R) or (**G**) siRNA-resistant ATF5 (ATF5-R) was used to rescue the siRNA effect. (**H**) Western blot analysis of HepG2 cells transfected with HPIP or HPIP plus mTOR siRNAs.

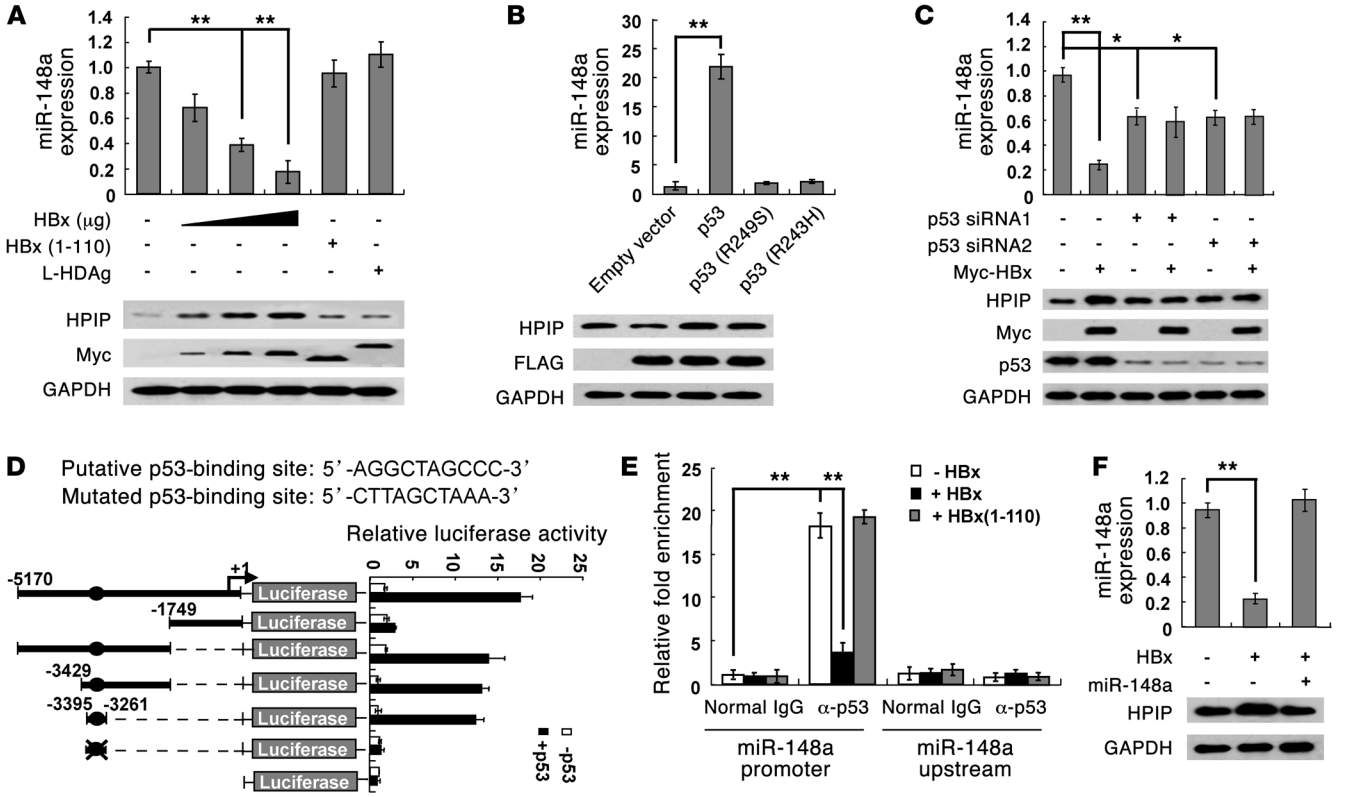

Figure 4

HBx inhibits p53-mediated activation of miR-148a and activates HPIP through repression of miR-148a. (**A**) HBx suppresses miR-148a expression and increases HPIP expression. LO2 cells were transfected with increasing doses of Myc-tagged HBx or Myc-tagged HBx(1–110) or L-HDAg and analyzed for miR-148a expression by real-time RT-PCR and for HPIP expression by immunoblot. (**B**) LO2 cells were transfected with FLAG-tagged p53, p53(R249S), or p53 (R273H) and analyzed as in **A**. (**C**) LO2 cells were transfected with Myc-tagged HBx and p53 siRNAs or control siRNA and analyzed as in **A**. (**D**) Luciferase activity of different promoter constructs in LO2 cells transfected with p53 or empty vector. The arrow indicates the position of the transcriptional start site. Filled circles show the position of the p53-binding site, and the "X" shows the mutated p53-binding site. (**E**) ChIP analysis of p53 occupancy on the miR-148a promoter in LO2 cells transfected with Myc-tagged HBx or HBx(1–110). (**F**) LO2 cells were transfected with HBx or HBx plus miR-148a and analyzed as in **A**. All values shown are mean ± SD of triplicate measurements and have been repeated 3 times with similar results (*$P < 0.05$, **$P < 0.01$).

targets through the mTORC2 signaling pathway, we knocked down Rictor, an essential component of mTORC2, in HepG2 cells with Rictor-specific siRNAs. As expected, Rictor knockdown decreased AKT phosphorylation at S473 but not T308 (Supplemental Figure 6, B and C). Importantly, knockdown of Rictor had little effect on miR-148a/HPIP modulation of mTORC1 targets. Taken together, these data suggest that miR148a/HPIP control the mTORC1/mTOR signaling pathway.

miR-148a/HPIP regulates mTOR expression through the AKT/ERK/FOXO4/ATF5 pathway. mTOR is a serine/threonine protein kinase that regulates cell proliferation, migration, and invasion. Our study demonstrates that miR-148a/HPIP modulates mTOR expression. A previous study has shown that the oncoprotein breakpoint cluster region–abelson (BCR-ABL) controls mTOR transcription in leukemia cells through the AKT/FOXO4/ATF5 pathway (22). BCR-ABL activates AKT, which in turn phosphorylates the transcription factor forkhead box O4 (FOXO4) and inactivates FOXO4. Inactivation of FOXO4 promotes the expression of activating transcription factor 5 (ATF5), one of whose transcriptional targets is mTOR. Activation of ERK1/2 has also been shown to phosphorylate FOXO proteins, resulting in negative regulation of FOXO transcriptional activity (23). As miR-148a/HPIP regulates AKT and ERK1/2 activation, we hypothesized that miR-148a/HPIP may modulate mTOR expression through the AKT/ERK/FOXO4/ATF5 pathway. As expected, miR-148a inhibited mTOR transcription in HepG2 cells (Figure 3A). HPIP reexpression in miR-148a-HepG2 cells reversed the inhibition of miR-148a–mediated mTOR transcription, suggesting that miR-148a regulates mTOR transcription through HPIP inhibition. Moreover, HPIP overexpression increased mTOR transcription, whereas HPIP knockdown decreased mTOR transcription (Figure 3B). Importantly, in addition to the inhibition of AKT and ERK as well as mTOR expression, miR-148a reduced FOXO4 phosphorylation and ATF5 expression in HepG2 cells (Figure 3C). HPIP reexpression in miR-148a-HepG2 cells reversed the miR-148a–mediated effects. Furthermore, HPIP overexpression increased FOXO4 phosphorylation and ATF5 expression, and HPIP knockdown had opposite effects (Figure 3D).

To test whether HPIP regulates mTOR expression through modulation of AKT/ERK, FOXO4, and ATF5, we used LY294002 and PD98059 inhibitors or siRNAs for FOXO4 and ATF5 to inhibit AKT and ERK or knockdown FOXO4 and ATF5. Indeed,

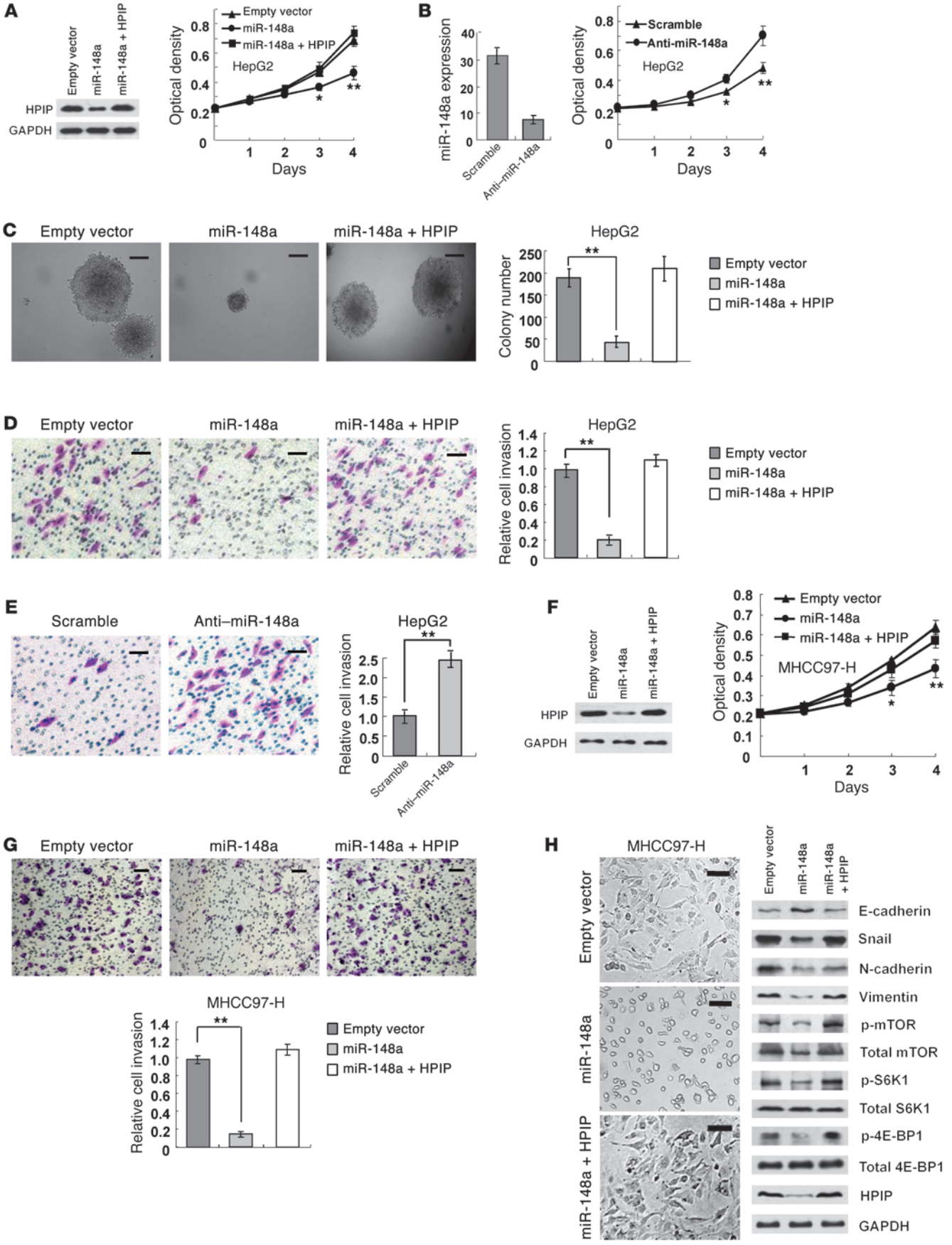
A
Empty vector
miR-148a
miR-148a + HPIP
HPIP
GAPDH
Optical density
Days
HepG2
B
miR-148a expression
Scramble
Anti-miR-148a
C
Colony number
D
Relative cell invasion
E
F
MHCC97-H
G
H
E-cadherin
Snail
N-cadherin
Vimentin
p-mTOR
Total mTOR
p-S6K1
Total S6K1
p-4E-BP1
Total 4E-BP1

Figure 5
miR-148a suppresses cell proliferation, migration, and invasion through inhibition of HPIP expression. (**A** and **B**) HepG2 cells expressing (**A**) miR-148a or miR-148a plus HPIP or (**B**) anti–miR-148a were cultured in regular medium. At specified times, cell numbers were determined by CCK-8 assay. The representative immunoblot (**A**, top panel) and real-time RT-PCR (**B**, top panel) show HPIP or miR-148a expression. (**C**) HepG2 cells expressing miR-148a or miR-148a plus HPIP were plated in soft agar and assayed for colony number after 3 weeks. Representative images show colonies in soft agar. Scale bar: 100 μM. (**D** and **E**) Cell invasion was evaluated in HepG2 cells expressing (**D**) miR-148a or miR-148a plus HPIP or (**E**) anti–miR-148a using a Matrigel invasion chamber. Invasive cells were fixed and stained with crystal violet (top panels). Scale bar: 100 μm. (**F**) MHCC97-H cells expressing miR-148a or miR-148a plus HPIP were analyzed as in **A**. (**G**) MHCC97-H cells expressing miR-148a or miR-148a plus HPIP were analyzed as in **D**. Scale bar: 100 μm. (**H**) Immunoblot analysis of MHCC97-H cells transfected with miR-148a or miR-148a plus HPIP. Morphologic changes are shown in the photographs. Scale bar: 100 μm. All values shown are mean ± SD of triplicate measurements and have been repeated 3 times with similar results (*$P < 0.05$, **$P < 0.01$).

inhibition of AKT or ERK abolished the ability of HPIP to increase FOXO4 phosphorylation and ATF5 expression (Figure 3E). FOXO4 knockdown abrogated the ability of HPIP to enhance the expression of ATF5 and mTOR (Figure 3F), and ATF5 knockdown abolished the ability of HPIP to promote mTOR expression (Figure 3G). These effects could be rescued by siRNA-resistant FOXO4 and ATF5 expression. Neither knockdown of FOXO4 nor knockdown of ATF5 altered the phosphorylation of AKT and ERK1/2 (Figure 3, F and G), and ATF5 knockdown did not change FOXO4 phosphorylation (Figure 3G). These data suggest that HPIP regulates mTOR expression through the AKT/ERK/FOXO4/ATF5 pathway.

To determine the role of mTOR in HPIP modulation of mTOR targets, we knocked down mTOR with mTOR siRNAs. Although HPIP increased phosphorylation of S6K1 and 4E-BP1 as well as the expression of c-myc and cyclin D1, mTOR knockdown abolished the ability of HPIP to regulate these mTOR targets (Figure 3H).

Taken together, our data suggest that the miRNA-148a/HPIP axis may control mTORC1 signaling by a cooperative mechanism, involving both modulation of upstream AKT/ERK signaling and mTOR expression.

HBx suppresses p53-mediated activation of miR-148a and activates HPIP through inhibition of miR-148a. HBx protein has been shown to play a key role in the molecular pathogenesis of HBV-related HCC (16, 17). To test whether HBx has an effect on miR-148a expression, we transfected normal human hepatocyte LO2 cells with HBx or its deletion mutant or large hepatitis delta antigen (L-HDAg). Expression of HBx, but not the C-terminal deletion mutant HBx(1–110) and L-HDAg, inhibited miR-148a expression, suggesting that HBx inhibition of miR-148a is specific (Figure 4A). Similar results were observed in HepG2 (Supplemental Figure 7A) and BEL-7402 (Supplemental Figure 7B) cells. Consistent with miR-148a inhibition of HPIP, HBx increased HPIP expression, whereas HBx(1–110) and L-HDAg had much less effect on HPIP expression than HBx (Figure 4A). The observation that HBx(1–110) and L-HDAg slightly increased HPIP expression raises the possibility that HBx(1–110) and L-HDAg may regulate HPIP expression through other mechanisms in addition to miR-148a. HBx did not alter the expression of B cell CLL/lymphoma 2 (*Bcl-2*) (Supplemental Figure 7C), another previously reported miR-148a target gene (24), suggesting that HBx selectively regulates miR-148 target gene expression.

HBx was reported to regulate gene expression through its interaction with host transcriptional factors, such as the tumor suppressor p53 (19, 25, 26). To determine how HBx controls the expression of miR-148a and HPIP, we first tested the effects of p53 on the expression of miR-148a and HPIP. Overexpression of wild-type p53 in LO2 cells increased expression of miR-148a and decreased that of HPIP (Figure 4B). The 2 p53 mutants, p53 (R249S) and p53 (R273H), which were identified in a variety of cancers, including HCC (27, 28), failed to regulate the expression of miR-148a and HPIP (Figure 4B). In contrast, knockdown of endogenous p53 decreased expression of miR-148a and increased that of HPIP (Figure 4C). Furthermore, knockdown of p53 reduced the ability of HBx to regulate the expression of miR-148a and HPIP (Figure 4C). Thus, we determined whether the interaction between HBx and p53 is important for HBx modulation of miR-148a and HPIP expression. p53 (R249S) and p53 (R273H), which did not change miR-148a and HPIP expression, reduced the interaction between p53 and HBx (Supplemental Figure 8A). Similarly, HBx(1–110) did not interact with p53 (Supplemental Figure 8B). These results suggest that the interaction between HBx and p53 is responsible for HBx modulation of miR-148a and HPIP expression.

To determine whether p53 directly transcribes miR-148a, we characterized a putative p53-binding site in the promoter of miR-148a. p53 robustly stimulated the activity of the luciferase reporter containing the putative p53-binding site but not the reporter with the mutated binding site or without the putative p53-binding site (Figure 4D). ChIP assay showed that p53 was recruited to the miR-148a promoter but not to a region approximately 2-kb upstream of the miR-148a promoter (Figure 4E). Importantly, expression of HBx, but not the HBx(1–110) that did not interact with p53, decreased the promoter occupancy of p53 (Figure 4E). Taken together, these data strongly suggest that HBx inhibits miR-148a transcription through reduced recruitment of p53 to the miR-148a promoter.

To test whether HBx increases HPIP expression through inhibition of miR-148a, we transfected LO2 cells with HBx, either with or without miR-148a. As expected, HBx stimulated HPIP expression (Figure 4F). Importantly, introduction of miR-148a reversed the effect of HBx on HPIP expression, suggesting that HBx activates HPIP through inhibition of miR-148a.

miR-148a suppresses liver cancer cell proliferation, migration and invasion in vitro through inhibition of HPIP expression. Since miR-148a regulates the mTOR pathway, which plays a key role in cancer development and progression (5–7), we examined the effect of miR-148a on the growth of HepG2, SMMC-7721, and BEL-7402 cells. Cell proliferation and colony formation assays revealed that overexpression of miR-148a reduced the proliferation of these cell lines (Figure 5A and Supplemental Figure 9), whereas miR-148a inhibition enhanced the proliferation of these cell lines (Figure 5B and Supplemental Figure 9). Overexpression of HPIP reversed the effect of miR-148a on HepG2 cell proliferation (Figure 5A). Soft agar assay showed that miR-148a inhibited anchorage-independent HepG2 cell proliferation (Figure 5C). Again, introduction of HPIP reversed the effect of miR-148a on anchorage-independent HepG2 cell proliferation (Figure 5C). These results suggest that miR-148a inhibits hepatoma cell proliferation by targeting HPIP.

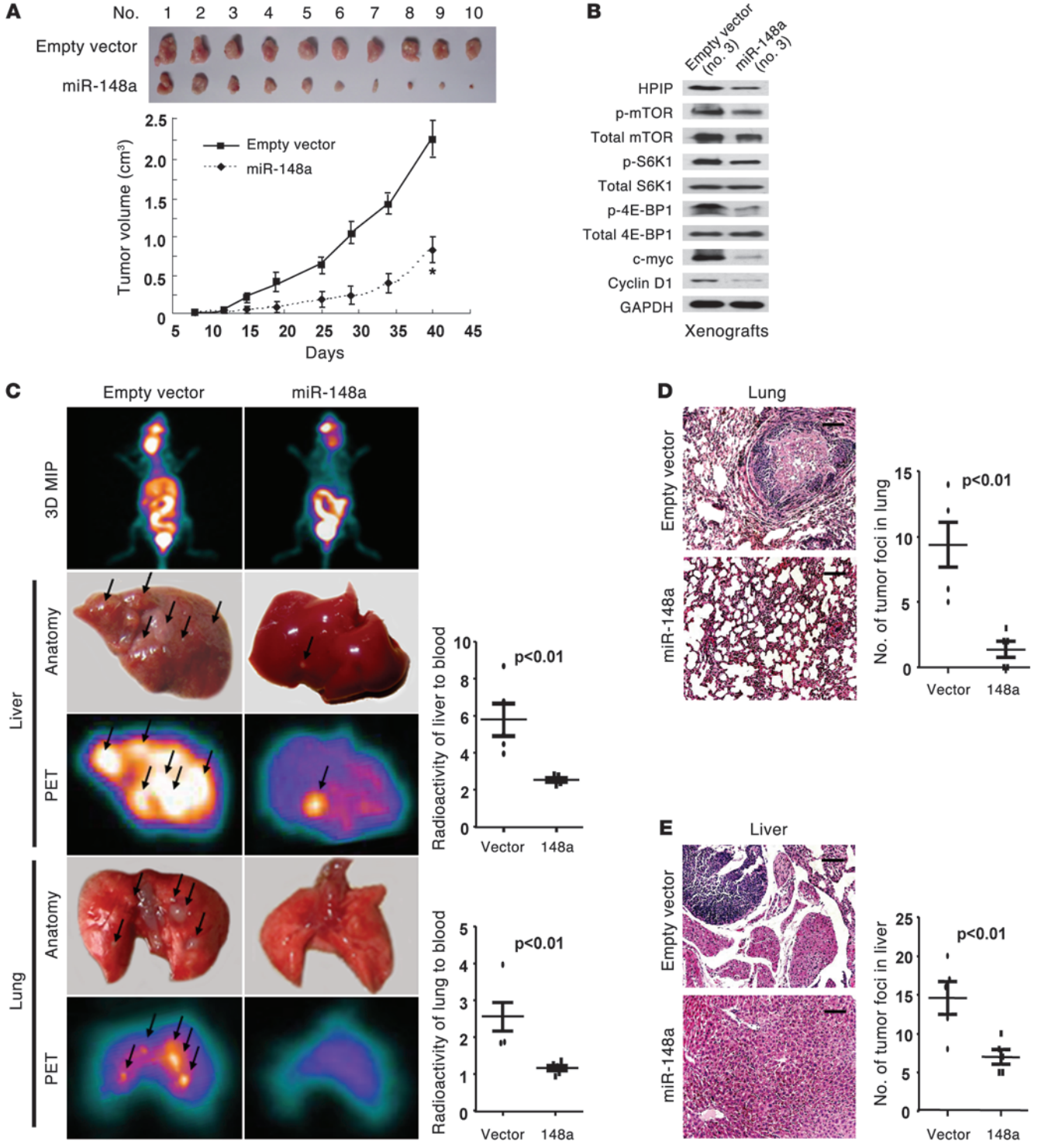

Figure 6

miR-148a reduces tumor growth and metastasis of HCC cell lines in nude mice. (**A**) HepG2 cells stably expressing miR-148a were injected into nude mice. At the indicated times, tumors were measured with Vernier calipers (mean ± SD; $n = 10$). *$P < 0.01$. (**B**) Immunoblot analysis of representative excised tumor from **A**. (**C**) FDG-PET images of a living mouse injected with miR-148a– or control vector–transfected MHCC97-H cells were collected ($n = 6$). Images and radioactivity of ablated livers and lungs show that miR-148a clearly repressed the number of the intrahepatic nodules and nodules spread throughout the pulmonary region. Arrows indicate tumor foci. 3D MIP, 3-dimensional maximum intensity projection. (**D** and **E**) Representative H&E-stained sections of the (**D**) lung and (**E**) liver tissues are shown. The number of tumor nodules was examined under an anatomical microscope. Scale bar: 100 μm. Symbols represent individual mice; horizontal bars indicate the mean ± SD.

Next, we examined the effects of miR-148a on migration and invasive capacity of hepatoma cells. miR-148a overexpression suppressed cell migration in HepG2, SMMC-7721, and BEL-7402 cells using a wound-healing assay (Supplemental Figure 10, A, C, and E). Matrigel invasion assays demonstrated that miR-148a overexpression decreased the number of invaded cells in these cell lines (Figure 5D and Supplemental Figure 10, G and H). Conversely, miR-148a inhibition had opposite effects (Figure 5E and Supplemental Figure 10, B, D, and F). HPIP reexpression in miR-148a-HepG2 cells reversed the effects of miR-148a on cell migration and invasion (Figure 5D and Supplemental Figure 10A). Importantly, similar results were observed in HBx-expressing MHCC97-H cells (Figure 5, F and G). Thus, we tested direct effects of miR-148a on HBx-mediated growth and migration of hepatocytes. As expected, HBx increased LO2 cell growth and migration (Supplemental Figure 11, A and B). Intriguingly, these effects were rescued by miR-148a reexpression. Similar effects were observed in HepG2 cells (Supplemental Figure 11, C and D). These data suggest that HBx enhances liver cell growth and migration through inhibition of miR-148a.

miR-148a inhibits EMT through inhibition of HPIP expression. Since EMT is well known to be involved in invasion and metastasis of cancer cells (29–31), we tested the effects of miR-148a on EMT in MHCC97-H cells. miR-148a overexpression inhibited morphologic changes from a polarized epithelial phenotype, which caused an elongated fibroblastoid phenotype (Figure 5H), suggesting that miR-148a suppresses EMT. Moreover, miR-148a increased expression of the epithelial marker E-cadherin and decreased that of the E-cadherin repressor Snail as well as N-cadherin and Vimentin, 2 mesenchymal markers, accompanied by the inhibition of mTOR signaling (Figure 5H). The observed miR-148a–mediated phenotype was rescued by HPIP overexpression. Moreover, miR-148a reversed HBx-mediated effects on EMT and mTOR signaling (Supplemental Figure 11E). miR-148a also inhibited EMT in HepG2 cells (Supplemental Figure 12, A and B). These results suggest that miR-148a may control HCC progression and metastasis through regulation of EMT.

miR-148a inhibits tumor growth and metastasis of HCC in nude mice. To confirm the in vitro phenotype of miR-148a expression, we first examined the effect of miR-148a on HepG2 cell growth in nude mice. miR-148a markedly suppressed tumor growth (Figure 6A). As expected, the tumors in mice inoculated with miR-148a-HepG2 cell lines had reduced levels of HPIP and phosphorylation of mTOR, S6K1, and 4E-BP1 and the mTOR effectors c-myc and cyclin D1 (Figure 6B).

Next, we used a HBx-expressing metastatic HCC cell line, MHCC97-H, which showed lung metastasis, to measure the effect of miR-148a on metastasis. The number of the intrahepatic nodules and nodules spread throughout the pulmonary region was clearly decreased in the miR-148a–expressing group compared with that in empty vector group (Figure 6C). In the 3-dimensional maximum intensity projection and PET images, lung-to-blood or liver-to-blood radioactivity in the miR-148a–expressing group was significantly lower than that in control group. Histologic analysis on the lungs and livers confirmed the metastasis foci (Figure 6, D and E). The number of tumor foci found in the lungs or livers in the miR-148a group was much lower than that in the empty vector group (Figure 6, D and E). These findings strongly supported the role of miR-148a as a suppressor of tumor dissemination.

HPIP increases hepatoma cell proliferation, migration, and invasion and promotes EMT through regulation of mTOR signaling. Since miR-148a exerts its function through inhibition of HPIP, we determined whether HPIP has opposite functions of miR-148a in the regulation of HCC cell proliferation, migration, and invasion as well as EMT. As expected, HPIP overexpression in HepG2 cells promoted cell proliferation (Figure 7A), accompanied by elevated levels of phosphorylation of mTOR, S6K1, and 4E-BP1 and increased expression of c-myc and cyclin D1 (Figure 7B). However, treatment with the mTOR inhibitor rapamycin abolished the ability of HPIP to regulate cell proliferation as well as the mTOR pathway molecules (Figure 7, A and B). A similar trend was obtained in migration and invasion assays (Figure 7, C and D). Contrary to results found with miR-148a, HPIP increased EMT, with enhanced expression of N-cadherin, Vimentin, and Snail and reduced expression of E-cadherin (Figure 7E). The observed EMT effects could be reversed by rapamycin, suggesting that HPIP promotes EMT through regulation of mTOR signaling. Moreover, HPIP knockdown had similar effects to miR-148a overexpression on the regulation of hepatoma cell proliferation, invasion, and EMT and abolished the ability of miR-148a to regulate these effects (Supplemental Figure 12, C–E). The knockdown effects could be rescued by siRNA-resistant HPIP expression. These data indicate that HPIP is a key mediator of miR-148a function. In addition, AKT and ERK1/2 were required for miR-148a/HPIP modulation of EMT because inhibition of AKT and ERK1/2 abolished the ability of miR-148a/HPIP to regulate EMT (Supplemental Figure 13).

Expression of miR-148a and HPIP and correlation among miR-148a, HPIP, and HBV infection in human HCC samples. First, we assessed the miR-148a expression levels in a HCC cohort consisting of 52 pairs of primary HCC and their corresponding nontumorous livers by real-time RT-PCR. Compared with their corresponding nontumorous counterparts, miR-148a expression was reduced in liver cancer tissues ($P = 7.70 \times 10^{-8}$) (Figure 8A and Supplemental Figure 14A). Interestingly, expression levels of miR-148a in patients with HBV infection with HCC (43 cases) were lower than those in patients without HBV infection with HCC (9 cases) ($P = 5.32 \times 10^{-7}$), indicating that HBV infection may lead to reduced miR-148a expression (Figure 8B).

Next, we used Western blot and immunohistochemistry to detect HPIP protein expression in 52 pairs of HCC tumors and matched nontumor liver tissues. Western blot analysis demonstrated that 47 out of 52 (90.4%) of HCC cases had upregulated HPIP expression (Supplemental Figure 14B). Moreover, immunohistochemical staining showed that HPIP expression was upregulated in HCC tissues ($P = 2.10 \times 10^{-8}$) (Figure 8C), and patients with HBV infection with HCC had increased levels of HPIP compared with patients without HBV infection with HCC ($P = 3.78 \times 10^{-7}$) (Figure 8D), suggesting that HBV infection may cause increased HPIP expression. We confirmed the specificity of the HPIP antibody by immunohistochemical staining of HCC samples incubated with anti-HPIP preincubated with its antigen (Supplemental Figure 14C) and immunoblotting of lysates from HepG2 or LO2 cells transfected with HPIP siRNA (Supplemental Figure 14D). In agreement with miR-148a inhibition of HPIP in cultured cells, expression of miR-148a negatively correlated with HPIP expression in HCC samples ($P = 2.95 \times 10^{-10}$, $r = -0.609$) (Figure 8E). Together, these data strongly suggest important pathological roles of miR-148a and HPIP in HCC.

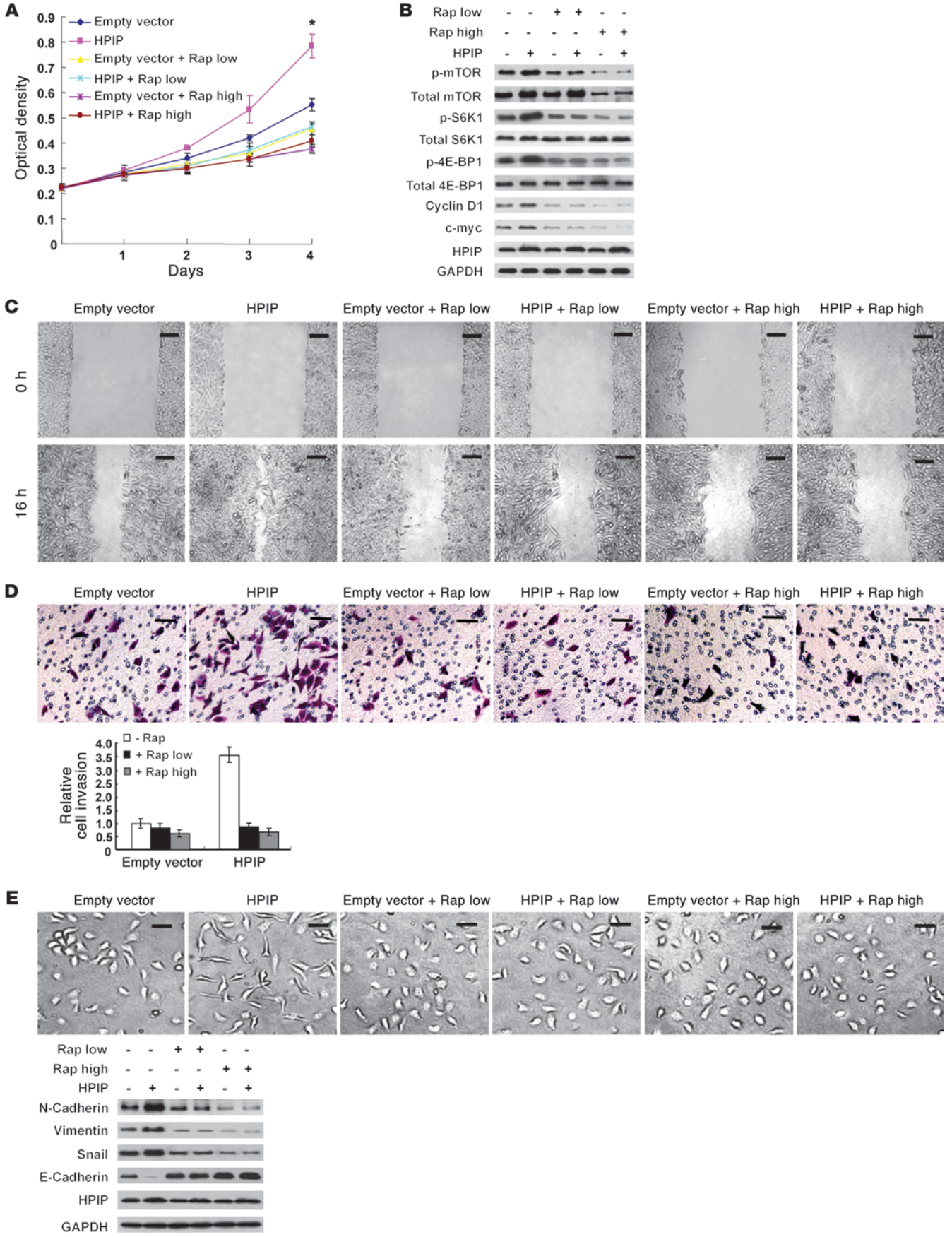
A
Empty vector
HPIP
Empty vector + Rap low
HPIP + Rap low
Empty vector + Rap high
HPIP + Rap high
Optical density
Days
B
Rap low
Rap high
HPIP
p-mTOR
Total mTOR
p-S6K1
Total S6K1
p-4E-BP1
Total 4E-BP1
Cyclin D1
c-myc
HPIP
GAPDH
C
Empty vector
HPIP
Empty vector + Rap low
HPIP + Rap low
Empty vector + Rap high
HPIP + Rap high
0 h
16 h
D
Empty vector
HPIP
Empty vector + Rap low
HPIP + Rap low
Empty vector + Rap high
HPIP + Rap high
- Rap
+ Rap low
+ Rap high
Relative cell invasion
Empty vector
HPIP
E
Empty vector
HPIP
Empty vector + Rap low
HPIP + Rap low
Empty vector + Rap high
HPIP + Rap high
Rap low
Rap high
HPIP
N-Cadherin
Vimentin
Snail
E-Cadherin
HPIP
GAPDH

Figure 7
HPIP increases hepatoma cell proliferation, migration, and invasion through regulation of mTOR signaling. (**A**) Cell proliferation assay for HepG2 cells transfected with HPIP or empty vector. Cells were treated with 20 nM or 200 nM rapamycin (Rap low or Rap high, respectively) for 24 hours. After 24 hours, the culture medium was changed to fresh drug-free medium, and cells were grown for the indicated times. (**B**) Western blot analysis of HepG2 cells from **A**. (**C**) Wound healing and (**D**) invasion assays for HepG2 cells transfected with HPIP or empty vector and treated with rapamycin for 24 hours or the indicated times. Scale bar: 100 μm. (**E**) Immunoblot analysis of HepG2 cells transfected with HPIP or empty vector and treated with rapamycin for 24 hours. Morphologic changes are shown in the photographs. Scale bar: 100 μm. All values shown are mean ± SD of triplicate measurements and have been repeated 3 times with similar results (*$P < 0.01$).

Discussion

We have demonstrated for the first time to our knowledge that the miR-148a/HPIP/mTOR pathway controls the growth and metastasis of HBV-related HCC (Figure 8F). The HBV-encoded protein HBx, which has been associated with the development and progression of HCC, inhibits p53-mediated induction of miR-148a through its interaction with p53. Inhibition of miR-148a leads to increased HPIP expression and subsequent activation of the mTOR pathway, which plays a critical role in tumor development, invasion, and metastasis. As expected, miR-148a inhibits the growth, EMT, invasion, and metastasis of HBx-expressing hepatoma cells through suppression of HPIP-mediated mTOR pathway. Moreover, expression of miR-148a is downregulated in patients with HBV-related liver cancer and negatively correlated with HPIP, which is upregulated in patients with HCC. We believe that these findings provide novel mechanistic insights into HBV-related hepatocarcinogenesis and metastasis.

Recently, Yuan et al. reported that anti–miR-148a inhibited the growth and migration of HBx-expressing hepatoma cells and that HBx increased miR-148a expression (32). Consistent with the results reported by Yuan et al., we also demonstrated that miR-148a expression was downregulated in HCC tissue as compared with nontumorous liver tissue. However, we obtained opposing conclusions regarding HBx modulation of miR-148a expression as well as miR-148a modulation of liver cancer cell growth and migration. The discrepancies between results of our study and those reported by Yuan et al. may be due to different liver cancer cell lines, sample size, and experimental strategies. First, Yuan et al. performed all experiments using HepG2 and Hep3B hepatoma cell lines stably overexpressing chloramphenicol acetyltransferase (CAT) or HBx, without parental cell lines as controls. We conducted experiments using parental HepG2, SMMC-7721, BEL-7402, and MHCC97-H hepatoma cells as well as the normal liver cell line LO2. Second, the expression levels of HBx in HBx stably transfected HepG2 and Hep3B cells used by Yuan et al. were not shown. Although they described that HBx can increase the expression of upregulated gene 11 (*URG11*), we do not see significant changes in the URG11 expression between HepG2 cells, presumably expressing CAT and HBx, according their Figure 7. We detected HBx expression in every experiment performed. Third, we performed both knockdown and overexpression experiments to determine the biological function of miR-148a, whereas Yuan et al. conducted only knockdown experiments with anti–miR-148a. For cell growth and migration assays, the knockdown effects with anti–miR-148a in their study are unknown, due to lack of the data. We showed the expression levels of miR-148a in the cell growth and migration experiments. Finally, we investigated clinical correlation in 43 patients with HBV infection with HCC and 9 patients without HBV infection with HCC. Yuan et al. assessed clinical correlation in 19 patients with HBV infection with HCC.

More recently, miRNA expression profiling studies have shown that HBx expression or HBV infection result in alterations of expression of many miRNAs, although the function of these miRNAs remains largely unknown (11, 33, 34). We identified miR-148a as a downstream target of HBx. Intriguingly, like HBx, HBV surface antigen (HBsAg) and HBV core antigen (HBcAg), 2 other HBV-encoded proteins, also inhibited miR-148a expression (data not shown). HBsAg indicates current hepatitis B infection and HBcAg is an indicator of active viral replication. The fact that HBsAg and HBcAg regulate miR-148a expression suggests that miR-148a may play a role in viral infection. The mechanisms by which HBsAg and HBcAg modulate miR-148a expression remain to be investigated. It will also be interesting to examine whether other tumor viruses alter host miR-148a expression.

Loss of function of the p53 tumor suppressor protein has been reported to be a causative event in the pathogenesis of a large fraction of human cancers (35–37). p53 is frequently mutated in human cancers, including HCC, and many mutations of p53 lead to loss of p53 function. Indeed, our study showed that, unlike wild-type p53, which induced miR-148a expression through binding to the miR-148a promoter, p53(R249S) and p53(R273H) failed to stimulate miR-148a expression, suggesting that loss of p53 function represents a novel mechanism for miR-148a downregulation in patients with cancer. Another known mechanism underlying miR-148a downregulation is aberrant hypermethylation of the miR-148a promoter (38–40). HBx has been shown to interact with the transcription factor p53 and repress p53 transcriptional activity (25, 26). Although our data showed that HBx inhibits p53-mediated induction of miR-148a, we can not exclude the possibility that HBx may repress miR-148a transcription through interaction with other transcription factors.

miR-148a expression has been found to be downregulated in various types of nonvirus-associated cancers, including gastric cancer (16), colorectal cancer (16), and pancreatic ductal adenocarcinoma (17). In gastric cancer, miR-148a represses tumor cell invasion and metastasis by downregulating Rho-associated, coiled-coil containing protein kinase 1 (ROCK1), a key modulator of processes involving cytoskeletal rearrangement (41). miR-148a inhibits pancreatic cancer cell growth by targeting cell division cycle 25B (CDC25B), a key regulator for entry into mitosis (17). By silencing Bcl-2, an important apoptosis regulator, miR-148a induces apoptosis in colorectal cancer (24). We showed that miR-148a suppressed the growth, invasion, and metastasis of HBx-expressing hepatoma cells by directly targeting HPIP, whose role in human patients with cancer remains unknown. These data suggest that miR-148a plays important roles in the development and progression of both virus- and nonvirus-associated cancers. Although Bcl-2 is a direct target of miR-148a and HBx represses miR-148a expression, HBx fails to regulate Bcl-2 expression, indicating that HBx selectively regulates miR-148a target gene expression. We showed that miR-148a directly targets HPIP and HBx activates HPIP through inhibition of miR-148a. HPIP is overexpressed in patients with HBV-related liver cancer and reverses the tumor suppressive function of miR-148a. HPIP increases hepatoma cell proliferation, migration, and invasion through regulation of mTOR signaling. These data sug-

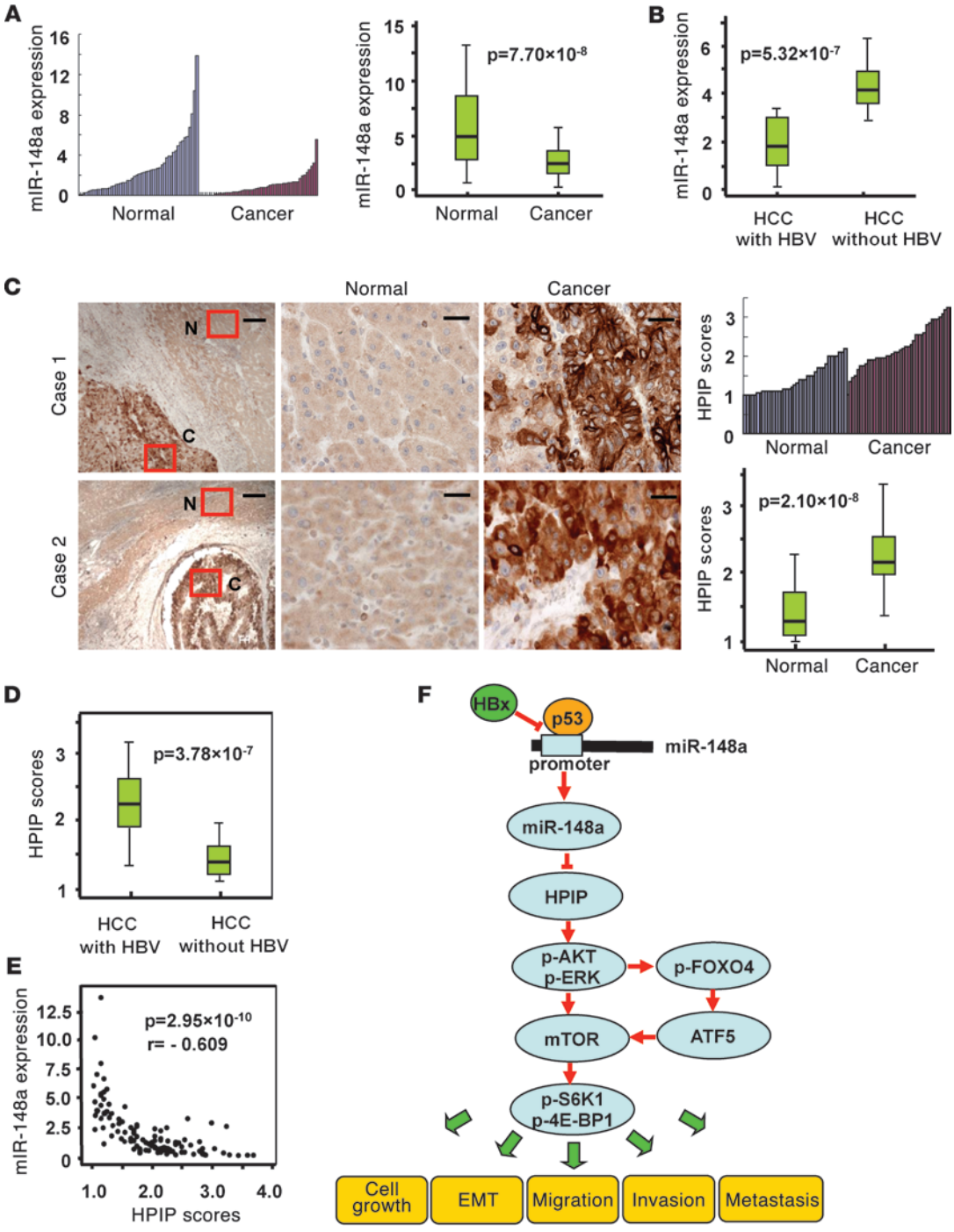

Figure 8

Expression of miR-148a and HPIP and their correlation in patients with liver cancer. (**A**) miR-148a expression in human cancerous liver tissues and adjacent normal liver tissues was plotted using real-time RT-PCR. The Mann-Whitney *U* test was used for comparison of cancer tissues with normal tissues ($n = 52$). (**B**) Comparison of expression levels of miR-148a in patients with HCC with and without HBV infection (independent *t* test). (**C**) Representative immunohistochemical staining of HPIP in cancerous (C) liver tissues and adjacent normal (N) liver tissues. The boxed areas in the left images are magnified in the middle and right images. Scale bar: 250 μm (left), 50 μm (middle and right). HPIP expression scores were plotted and compared (Mann-Whitney *U* test). (**D**) Comparison of HPIP scores in patients with HCC with and without HBV infection (independent *t* test). (**E**) The relationship between miR-148a and HPIP expression was detected by Spearman rank correlation analysis in liver samples. Symbols represent individual samples. (**F**) Proposed model for the HBx/miR-148a/HPIP/mTOR pathway that regulates cell growth, EMT, migration, invasion, and metastasis of HCC. In box-and-whisker plots, horizontal bars indicate the medians, boxes indicate 25th to 75th percentiles, and whiskers indicate 10th and 90th percentiles.

gest that HPIP is a key mediator of virus-related carcinogenesis and progression. Although HPIP upregulation in patients with cancer may be due to miR-148a downregulation, we can not exclude other mechanisms. EMT is an important step toward tumor invasion and metastasis. EMT can be induced by a variety of different molecules and pathways, including AKT (42), ERK (43, 44), and mTOR signaling (45–47), all of which are commonly deregulated in human cancers (5, 48, 49). Since miR-148a and HPIP are upstream regulators of AKT, ERK, and mTOR signaling, we believe that miR-148a and HPIP are critical regulators of EMT. The important role of miR-148a and HPIP in cancer suggests that miR-148a activation or HPIP inhibition may be a useful strategy for cancer treatment.

Methods

Plasmids, cell lines, and reagents. miRNA precursors of hsa-miR-148a, hsa-miR-148b, and hsa-miR-152 were gifts from Xiaofei Zheng. The miRNA precursor sequences were cloned into pcDNA3.0 vector (Invitrogen). miR-148a inhibitor (anti–hsa-miR-148a), which was chemically synthesized, single-stranded, modified RNA, was purchased from Qiagen. Wild-type and mutated miR-148a putative targets on HPIP 3′-UTR were cloned into pmirGLO dual-luciferase miRNA target expression vector (Promega). Briefly, the 3′-UTR of human *HPIP* gene was obtained by PCR using the following primers: 5′-CGGAATTCACCACCACCACCACCGGGGCTGA-3′ (forward) and 5′-GCTCTAGAGCAGGTCCAGCTAAGGCCTTTTTCT-3′ (reverse). To introduce mutations into the seed sequences of the predicted miR-148a target sites within the HPIP 3′-UTR, recombinant PCR was performed using the above-mentioned primers and the following primers: 5′-GACTGTACGGGCTGGTGATTTTGCTCTACTGTGTGAAAG-3′ (forward) and 5′-CACACAGTAGAGCAAAATCACCAGCCCGTACAGTCTG-3′ (reverse). The 3′-UTR of the human *MTOR* gene was obtained by PCR using the following primers: 5′-CCGCTCGAGAGATGTGCCCATCACGTT-3′ (forward) and 5′-GCTCTAGACTGATGTCATTTATTGGCACA-3′ (reverse). After construction of the luciferase reporter genes, DNA sequences of the 3′-UTR were verified. Expression vectors for p53 siRNAs were from Yi Song. Expression plasmids for FOXO4 siRNAs (50), ATF5 siRNAs (51), mTOR siRNAs (52, 53), and Rictor siRNAs (54) have been previously described. Expression vectors for HPIP and HPIP siRNA1 have been previously described (12). The cDNA target sequence of HPIP siRNA2 was TTCTAGGGAGTGGAGTGGA. Expression constructs for siRNA-resistant HPIP, FOXO4, or ATF5 were generated by recombinant PCR, with a silent mutation in the 3′ nucleotide of a codon in the middle of the siRNA-binding site. The coding sequences of full-length HBx and its deletion mutant were amplified by PCR using pHBV3091 as a template (55) and cloned into pXJ40 vector harboring Myc epitope sequence (pXJ40-Myc). All cell lines (with wild-type p53) were purchased from ATCC but the MHCC97-H cell line (with mutant p53 at codon 249), which was a gift from Ying Jiang (56). Stable cell lines overexpressing miR-148a were generated by lentiviral transduction using pCDH plasmid carrying miR-148a (System Biosciences). Anti–cyclin D1, anti-ERK1/2, anti-AKT, anti–p-AKT(T308), anti–p-AKT(S473), anti–p-ERK1/2(T202/Y204), and anti-ATF5 antibodies were purchased from Santa Cruz Biotechnology Inc.; anti–E-cadherin, anti-Snail, and anti–N-cadherin were obtained from BD Biosciences; anti-mTOR, anti–p-mTOR(S2448), anti-S6K1, anti–p-S6K1(T389), anti–4E-BP1, anti–p-4E-BP1(T37/46), anti-Vimentin, and anti–p-FOXO4(S193) were from Cell Signaling Technology; and anti-HPIP and anti-FOXO4 antibodies were obtained from Proteintech.

Luciferase reporter assay. Cells seeded into 24-well plates were cotransfected with miR-148a and luciferase reporter constructs containing wild-type or mutated HPIP 3′-UTR. Cells were harvested and analyzed for luciferase and β-galactosidase activities, as described previously (57). All transfection experiments were performed in triplicate and reproduced at least 3 times.

miRNA extraction and quantitative RT-PCR. Total RNA from tissues or cell lines containing miRNA was extracted using the miRNeasy Mini kit (Qiagen). Target miRNA was reverse transcribed to cDNA by a gene-specific RT primer using the miScript Reverse Transcription Kit (Qiagen). miRNA expression profiles of tissues or cell lines were determined with miScript SYBR Green PCR Kit (Qiagen) and performed on ABI7000 Real-Time PCR System (Applied Biosystems). Analysis of *MTOR* mRNA expression by quantitative RT-PCR (qRT-PCR) was performed, as previously described (22). The relative quantification value of the target, normalized to a control, was calculated by the comparative Ct methods. The products of qRT-PCR were verified by sequencing.

ChIP. ChIP assay was performed with LO2 cells transfected with HBx or empty vector using the Magna ChIP Assay Kit (Millipore) according to the manufacturer's instructions (58). Protein-DNA complexes were precipitated with normal IgG and anti-p53 (Sigma-Aldrich) at 4°C overnight with rotation. PCR was performed with the following primers: miR-148a promoter sense, 5′-GCCAGCTATCTTTCCACATCTGC-3′; miR-148a promoter antisense, 5′-CGCAGCCCCTAAAATATGCTTCTG-3′; miR-148a upstream sense, 5′-GTATTTCCTTTCTAGATAATAACTATAAC-3′; miR-148a upstream antisense, 5′-CTATCACTGATGGTGATAATCTACATC-3′.

Cell growth and colony formation assays. Anchorage-dependent cell growth was assessed by the CCK-8 Kit (Dojindo Laboratories) according to the manufacturer's instructions. For colony formation assay, transfected cells were seeded in 6-well plates at 2,000 cells per well. Two weeks later, colonies were fixed with 4% paraformaldehyde and stained with crystal violet for 30 minutes. The number of colonies with diameters of more than 1.5 mm were counted. For anchorage-independent growth assay (59), transfected cells were seeded in 6-cm plates, with a bottom layer of 0.7% low-melting-temperature agar in DMEM and a top layer of 0.35% agar in DMEM. Colonies with diameters greater than 100 μm were scored after 3 weeks of growth.

Cell migration and invasion assays. Wound healing assays were used to determine cell migration. Briefly, transfected cells grown in 6-well plates as confluent monolayers were mechanically scratched using a 1-ml pipette tip to create the wound. Cells were washed with PBS to remove the debris and were cultured for 16 hours to allow wound healing. Cell invasion assay was performed with Matrigel (BD Biosciences) coated on the upper surface of the transwell chamber (Corning). Twenty-four hours later, cells invaded through the Matrigel membrane were fixed with 4% paraformaldehyde and stained with crystal violet. After taking photographs, the number of invaded cells was counted.

In vivo tumor growth and metastasis. Animal studies were approved by the Institutional Animal Care Committee of Beijing Institute of Biotechnology. For in vivo tumor growth assay, HepG2 cells stably infected with pCDH or pCDH-miR-148a were injected subcutaneously in the dorsal of each animal (6-week-old male nude mice), respectively (n = 10). Tumor size was measured at indicated times (see Figure 6A) using calipers. Tumor volume was calculated according to the following formula: volume = (longest diameter × shortest diameter^2)/2. For the metastasis model, 2×10^6 MHCC97-H cells stably transfected with pCDH control or pCDH-miR-148a were injected intravenously via the lateral tail vein (n = 6). All mice were kept for about 60 days until imaged by small-animal PET imaging.

Small-animal PET imaging. PET of tumor-bearing mice was performed using an animal PET scanner (Philips Corp.). After they were intraperitoneally anesthetized by pentobarbital (100 mg/kg), mice were injected intravenously with 3.7 MBq (100 μCi) of ^{18}F radio-labeled fluorodeoxyglucose (^{18}F-FDG). Five-minute emission scans were performed to obtain attenuation correction data in the prone position at 60 minutes after injection, and delay scans of 10 minutes were acquired at 2 hours. The radioactivity of organs and blood was measured using a NaI (Tl) well counter (China Atom Corp.). For each mouse, radioactivity was calibrated against a known aliquot of the injected tracer and presented as percent injected dose of tissue.

Clinical samples and immunohistochemistry. Fifty-two pairs of liver tumor samples and adjacent noncancerous tissues were obtained from the Chinese PLA General Hospital, with the informed consent of patients and with approval for experiments from the Chinese PLA General Hospital and Beijing Institute of Biotechnology. Tissue samples were used for miRNA and protein extraction as well as immunohistochemistry analysis. Immunoblot and immunohistochemistry analyses were performed as previously described (58, 59). All immunohistochemistry staining was assessed by pathologists blinded to the origination of the samples. The widely accepted H-score system was used in considering the staining intensity and extent of staining area. Briefly, H-score was generated by adding the percentage of strongly stained cells (times 3), the percentage of moderately stained cells (times 2), and the percentage of weakly stained cells (times 1).

Statistics. Differences between variables were assessed by χ^2 analysis, 2-tailed Student's *t* test, or Mann-Whitney *U* test. Statistical calculations were performed using SPSS 13.0. *P* values of less than 0.05 were considered statistically significant.

Acknowledgments

This work was supported by Major State Basic Research Development Program (2011CB504202, 2012CB945100, and 2009CB521804), National Natural Science Foundation (81072173, 31100604, 81101065, 30625035, and 30530320), and National Key Technologies R&D Program for New Drugs (2009ZX09301-002).

Received for publication November 13, 2012, and accepted in revised form November 21, 2012.

Address correspondence to: Qinong Ye, Department of Medical Molecular Biology, Beijing Institute of Biotechnology, 27 Tai-Ping Lu Rd., Beijing 100850, China. Phone: 8610.6818.0809; Fax: 8610.6824.8045; E-mail: yeqn66@yahoo.com. Or to: Nan Du, First Affiliated Hospital, Chinese PLA General Hospital, 51 Fu-Cheng Lu Rd., Beijing 100048, P. R. China. Phone: 8610.6898.9123; Fax: 8610.6898.9123; E-mail: dunan05@yahoo.com.cn.

1. Bartel D. MicroRNAs: genomics, biogenesis, mechanism, and function. *Cell*. 2004;116(2):281–297.
2. Calin GA, Croce CM. MicroRNA signatures in human cancers. *Nat Rev Cancer*. 2006;6(11):857–866.
3. Croce CM. Causes and consequences of microRNA dysregulation in cancer. *Nat Rev Genet*. 2009;10(10):704–714.
4. Zhang B, Pan X, Cobb GP, Anderson TA. microRNAs as oncogenes and tumor suppressors. *Dev Biol*. 2007;302(1):1–12.
5. Guertin DA, Sabatini DM. Defining the role of mTOR in cancer. *Cancer Cell*. 2007;12(1):9–22.
6. Dazert E, Hall MN. mTOR signaling in disease. *Curr Opin Cell Biol*. 2011;23(6):744–755.
7. Mendoza MC, Er EE, Blenis J. The Ras-ERK and PI3K-mTOR pathways: cross-talk and compensation. *Trends Biochem Sci*. 2011;36(6):320–328.
8. Moore PS, Chang Y. Why do viruses cause cancer? Highlights of the first century of human tumour virology. *Nat Rev Cancer*. 2010;10(12):878–889.
9. Saha A, Kaul R, Murakami M, Robertson ES. Tumor viruses and cancer biology: Modulating signaling pathways for therapeutic intervention. *Cancer Biol Ther*. 2010;10(10):961–978.
10. Lin Z, Flemington EK. miRNAs in the pathogenesis of oncogenic human viruses. *Cancer Lett*. 2011;305(2):186–199.
11. Zhang ZZ, et al. Hepatitis B virus and hepatocellular carcinoma at the miRNA level. *World J Gastroenterol*. 2011;17(28):3353–3358.
12. Wang X, et al. The estrogen receptor-interacting protein HPIP increases estrogen-responsive gene expression through activation of MAPK and AKT. *Biochim Biophys Acta*. 2008;1783(6):1220–1228.
13. Manavathi B, Acconcia F, Rayala SK, Kumar R. An inherent role of microtubule network in the action of nuclear receptor. *Proc Natl Acad Sci U S A*. 2006;103(43):15981–15986.
14. Abramovich C, et al. Functional cloning and characterization of a novel nonhomeodomain protein that inhibits the binding of PBX1-HOX complexes to DNA. *J Biol Chem*. 2000;275(34):26172–26177.
15. Cheng L, et al. PES1 promotes breast cancer by differentially regulating ERα and ERβ. *J Clin Invest*. 2012;122(8):2857–2870.
16. Chen Y, et al. Altered expression of MiR-148a and MiR-152 in gastrointestinal cancers and its clinical significance. *J Gastrointest Surg*. 2010;14(7):1170–1179.
17. Liffers ST, et al. MicroRNA-148a is down-regulated in human pancreatic ductal adenocarcinomas and regulates cell survival by targeting CDC25B. *Lab Invest*. 2011;91(10):1472–1479.
18. Neuveut C, Wei Y, Buendia MA. Mechanisms of HBV-related hepatocarcinogenesis. *J Hepatol*. 2010;52(4):594–604.
19. Ng SA, Lee C. Hepatitis B virus X gene and hepatocarcinogenesis. *J Gastroenterol*. 2011;46(8):974–990.
20. Pópulo H, Lopes JM, Soares P. The mTOR signalling pathway in human cancer. *Int J Mol Sci*. 2012;13(2):1886–1918.
21. Toschi A, Lee E, Xu L, Garcia A, Gadir N, Foster DA. Regulation of mTORC1 and mTORC2 complex assembly by phosphatidic acid: competition with rapamycin. *Mol Cell Biol*. 2009;29(6):1411–1420.
22. Sheng Z, Ma L, Sun JE, Zhu LJ, Green MR. BCR-ABL suppresses autophagy through ATF5-mediated regulation of mTOR transcription. *Blood*. 2011;118(10):2840–2848.
23. Roy SK, Srivastava RK, Shankar S. Inhibition of PI3K/AKT and MAPK/ERK pathways causes activation of FOXO transcription factor, leading to cell cycle arrest and apoptosis in pancreatic cancer. *J Mol Signal*. 2010;5:10.
24. Zhang H, et al. MiR-148a promotes apoptosis by targeting Bcl-2 in colorectal cancer. *Cell Death Differ*. 2011;18(11):1702–1710.
25. Dewantoro O, Gani RA, Akbar N. Hepatocarcinogenesis in viral Hepatitis B infection: the role of HBx and p53. *Acta Med Indones*. 2006;38(3):154–159.
26. Elmore LW, et al. Hepatitis B virus X protein and p53 tumor suppressor interactions in the modulation of apoptosis. *Proc Natl Acad Sci U S A*. 1997;94(26):14707–14712.
27. Staib F, Hussain SP, Hofseth LJ, Wang XW, Harris CC. TP53 and liver carcinogenesis. *Hum Mutat*. 2003;21(3):201–216.
28. Wong KB, DeDecker BS, Freund SM, Proctor MR, Bycroft M, Fersht AR. Hot-spot mutants of p53 core domain evince characteristic local structural changes. *Proc Natl Acad Sci U S A*. 1999;96(15):8438–8442.
29. Thiery JP, Acloque H, Huang RY, Nieto MA. Epithelial-mesenchymal transitions in development and disease. *Cell*. 2009;139(5):871–890.
30. Moreno-Bueno G, Portillo F, Cano A. Transcriptional regulation of cell polarity in EMT and cancer. *Oncogene*. 2008;27(55):6958–6969.
31. Christiansen JJ, Rajasekaran AK. Reassessing epithelial to mesenchymal transition as a prerequisite for carcinoma invasion and metastasis. *Cancer Res*. 2006;66(17):8319–8326.
32. Yuan K, Lian Z, Sun B, Clayton MM, Ng IO, Feitelson MA. Role of miR-148a in hepatitis B associated hepatocellular carcinoma. *PLoS One*. 2012;7(4):e35331.
33. Gao P, Wong CC, Tung EK, Lee JM, Wong CM, Ng IO. Deregulation of microRNA expression occurs early and accumulates in early stages of HBV-associated multistep hepatocarcinogenesis. *J Hepatol*. 2011;54(6):1177–1184.
34. Yip WK, et al. Carboxyl-terminal truncated HBx regulates a distinct microRNA transcription program in hepatocellular carcinoma development. *PLoS. One*. 2011;6(8):e22888.
35. Kruse JP, Gu W. Modes of p53 regulation. *Cell*. 2009;137(4):609–622.
36. Soussi T, Wiman KG. Shaping genetic alterations in human cancer: the p53 mutation paradigm. *Cancer Cell*. 2007;12(4):303–312.
37. Levine AJ, Momand J, Finlay CA. The p53 tumour suppressor gene. *Nature*. 1991;351(6326):453–456.
38. Lujambio A, et al. A microRNA DNA methylation signature for human cancer metastasis. *Proc Natl Acad Sci U S A*. 2008;105(36):13556–13561.
39. Pavicic W, Perkio E, Kaur S, Peltomaki P. Altered methylation at microRNA-associated CpG islands in hereditary and sporadic carcinomas: a methylation-specific multiplex ligation-dependent probe amplification (MS-MLPA)-based approach. *Mol Med*. 2011;17(7-8):726–735.
40. Hanoun N, et al. The silencing of microRNA 148a production by DNA hypermethylation is an early event in pancreatic carcinogenesis. *Clin Chem*. 2010;56(7):1107–1118.
41. Zheng B, et al. MicroRNA-148a suppresses tumor cell invasion and metastasis by downregulating ROCK1 in gastric cancer. *Clin Cancer Res*. 2011;17(24):7574–7583.
42. Grille SJ, et al. The protein kinase Akt induces epithelial mesenchymal transition and promotes enhanced motility and invasiveness of squamous cell carcinoma lines. *Cancer Res*. 2003;63(9):2172–2178.
43. Ellenrieder V, et al. Transforming growth factor beta1 treatment leads to an epithelial-mesenchymal transdifferentiation of pancreatic cancer cells requiring extracellular signal-regulated kinase 2 activation. *Cancer Res*. 2001;61(10):4222–4228.
44. Shin SY, Rath O, Zebisch A, Choo SM, Kolch W, Cho KH. Functional roles of multiple feedback loops in extracellular signal-regulated kinase and Wnt signaling pathways that regulate epithelial-mesenchymal transition. *Cancer Res*. 2010;70(17):6715–6724.
45. Lamouille S, Derynck R. Cell size and invasion in TGF-beta-induced epithelial to mesenchymal transition is regulated by activation of the mTOR pathway. *J Cell Biol*. 2007;178(3):437–451.
46. Pon YL, Zhou HY, Cheung AN, Ngan HY, Wong AS. p70 S6 kinase promotes epithelial to mesenchymal transition through snail induction in ovarian cancer cells. *Cancer Res*. 2008;68(16):6524–6532.
47. Smith AP, et al. A positive role for Myc in TGFβ-induced Snail transcription and epithelial-to-mesenchymal transition. *Oncogene*. 2009;28(3):422–430.
48. Manning BD, Cantley LC. AKT/PKB signaling: navigating downstream. *Cell*. 2007;129(7):1261–1274.
49. Sebolt-Leopold JS, Herrera R. Targeting the mitogen-activated protein kinase cascade to treat can-

cer. *Nat Rev Cancer*. 2004;4(12):937–947.
50. Ford J, Jiang M, Milner J. Cancer-specific functions of SIRT1 enable human epithelial cancer cell growth and survival. *Cancer Res*. 2005; 65(22):10457–10463.
51. Sheng Z, et al. A genome-wide RNA interference screen reveals an essential CREB3L2-ATF5-MCL1 survival pathway in malignant glioma with therapeutic implications. *Nat Med*. 2010;16(6):671–677.
52. Kim DH, et al. mTOR interacts with raptor to form a nutrient-sensitive complex that signals to the cell growth machinery. *Cell*. 2002;110(2):163–175.
53. Busch S, Renaud SJ, Schleussner E, Graham CH, Markert UR. mTOR mediates human trophoblast invasion through regulation of matrix-remodeling enzymes and is associated with serine phosphorylation of STAT3. *Exp Cell Res*. 2009; 315(10):1724–1733.
54. Zhang F, et al. mTOR complex component Rictor interacts with PKCζ and regulates cancer cell metastasis. *Cancer Res*. 2010;70(22):9360–9370.
55. Han J, et al. Hepatitis B virus X protein and the estrogen receptor variant lacking exon 5 inhibit estrogen receptor signaling in hepatoma cells. *Nucleic Acids Res*. 2006;34(10):3095–3106.
56. Li Y, et al. Establishment of cell clones with different metastatic potential from the metastatic hepatocellular carcinoma cell line MHCC97. *World J Gastroenterol*. 2001;7(5):630–636.
57. Ding L, et al. Ligand-independent activation of estrogen receptor alpha by XBP-1. *Nucleic Acids Res*. 2003;31(18):5266–5274.
58. Ding L, et al. Human four-and-a-half LIM family members suppress tumor cell growth through a TGF-β-like signaling pathway. *J Clin Invest*. 2009;119(2):349–361.
59. Ding L, et al. FHL1 interacts with oestrogen receptors and regulates breast cancer cell growth. *J Cell Mol Med*. 2011;15(1):72–85.